

COMPARATIVE EVALUATION OF RCC & CONCRETE FILLED DOUBLE-SKIN STEEL TUBE BUILDING SUBJECTED TO STATIC AND DYNAMIC LOADING

Harsh G. Vaghasiya¹, Vishal B. Patel², Indrajit N. Patel³

M.Tech., Structural Engineering, Birla Vishvakarma Mahavidyalaya, Vallabh Vidyanagar, India¹

Assistant Professor., Structural Engineering, Birla Vishvakarma Mahavidyalaya, Vallabh Vidyanagar, India²

Professor & Principal, Birla Vishvakarma Mahavidyalaya, Vallabh Vidyanagar, India³

Abstract: The concrete-filled double skin steel tube (CFDST) is a unique steel-concrete composite construction that consists of two steel layers with a concrete layer in between. The inner hollow steel section serves as formwork and concrete reinforcement. Concrete prevents local buckling in hollow steel sections, increasing the section's ductility. CFDST has a number of benefits, including high strength, bending stiffness, and earthquake and fire resistance. Because of the large confinement effect, the circular CFDST column outperforms all other shapes for all parameters. Among all the literatures present, they have not studied the response to combine axial loading, moments and torsion, in this paper a building located at Vallabh Vidyanagar city was selected as the study frame and RCC column of that frame was taken as economical for given loadings. All the columns of this study frame were then replaced by equivalent CFDST columns and then by CFST columns (both circular sections) based on FE analysis results after analysing both the section in ABAQUS software. Performance evaluation of all three frames then carried out and compared. From that we can say that the forces which were present in the RCC or CFST section were reduced by significant amount which says that CFDST column's performance is better than both RCC and CFST columns under static loadings. The seismic performance of CFDST column section was found better than RCC frame or CFST frame under four different time-history analysis with that we can say that CFDST column can be used as an improvement over RCC or CFST column section.

Keywords: Circular Column, Composite Columns, Concrete-filled double skin steel tubes (CFDST), Comparative Study, Finite element analysis,

I. INTRODUCTION

Conventional RCC members like beams and columns are widely used for the construction. For increased load carrying capacity the use of composite columns is introduced. It combines the advantages of both steel and concrete. Steel-concrete composite columns have been widely used in modern construction industry owing to their high performance in terms of ductility, strength, energy absorption capacity as well as good constructability in comparison with reinforced concrete columns. In a concrete-filled steel tubular (CFST) column, concrete prevents the steel tube from the inward local-buckling and the steel tube acts as the permanent formwork for the concrete so that the construction cost and time can be greatly

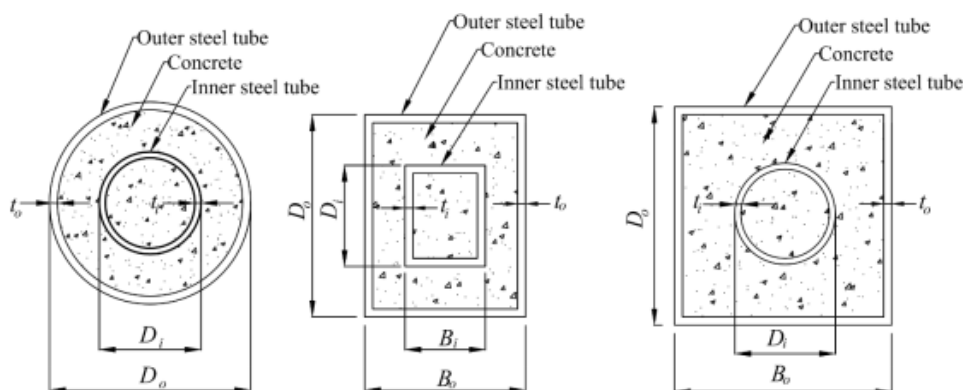


Fig. 1 Typical Cross-Sections of CFDST column

minimized. The concrete-filled double steel tubular (CFDST) column is an innovative form of composite columns where the steel tubes are placed concentrically and filled with concrete.

The choice of the cross-section and geometry of a CFDST column for a specific project is dependent on the structural efficiency of the column, specific architecture or aesthetic criteria, material availability or the cost and method of construction. As an example, circular CFDST columns have higher ductility and strength than rectangular CFDST columns. Rectangular CFDST columns offer ease of connection to the steel beams and can be used in the case where the large bending stiffness is essential. Square CFDST columns composed of an internal circular tube combine the benefits of both circular and square CFST columns. The presence of the internal circular tube improves the strength, ductility and fire-resistance of CFDST columns compared to CFST columns. Most popular failure modes (figure) of thin shell structures are Elephant foot buckling, Diagonal outward buckling and Distorted diamond shaped buckling which decides the capacity of section and behaviour of them when subjected to loading.

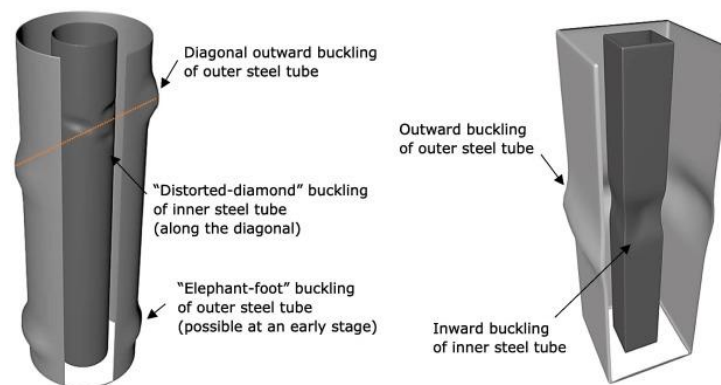


Fig. 2 Failure Patterns of CFDST column

II. LITERATURE REVIEW

1. M.F. Hassanein et al (2014) studied the behaviour concrete filled double skin steel tubular column with lean duplex stainless steel (EN 1.4162) material. The behavioral difference between an intermediate length and very long CFDST column in studied and suggested that the numerical expressions given in the Eurocode gives suitable results but not reliable due to over estimation of the strength of the CFDST column.
2. Vishal V. Gore et al (2016) studied the seismic behaviour of a RCC multistoried building provided with RCC and CFST columns. The results indicate that the building with CFST columns gives better performance against seismic forces. It was noted that there was a 40% reduction in the cross-sectional area used by CFST columns. There was also a considerable amount of reduction in the base shear values and in the lateral displacements of buildings with a reduction of nearly 18% of the buildings dead weight which proves to be useful in case of seismic studies.
3. M.F. Hassanein et al (2018) carried out analytical study concrete-filled double-skin short columns under compression. CFDST with square hollow section as inner and outer steel tube was taken. Parametric studies were done to investigate the effect of key parameters affecting the behaviour of CFDST column. The results indicated that variation in the hollow ratio is the best way to vary the axial load carrying capacity of the CFDST column rather than variation in the material strength or thickness of steel tube sections.
4. H. Saberi et al (2020) investigated the effect of concrete compressive strength on the axial performance of CFDST columns. The effects of concrete with different compressive strength, concrete confinement, bearing capacity and width-to-thickness ratio on the overall strength of tubular cross-section columns in their inner and outer skins are investigated.
5. Zhan Guo et al (2020) experimentally studied the compressive behaviour of square CFDST short columns with double internal steel tubes. The influence of concrete strength, eccentricity ratio, and section hollow ratio on the strength, deformation, and ductility was investigated. Comparisons of the experimental ultimate strength with three different design methods were made and simplified formulae were proposed to estimate the ultimate strength of CFDST short columns.

III. PROBLEM DISCRIPTION

An existing building model situated in Vallabh Vidyanagar as BVM girl's hostel is considered here for the study purpose. The details of this model and loadings are given in table below.

TABLE I Details of Building Modal

Number of stories	4
Story height	3.15 m
Size of beam	300mm X 600mm
Size of column	300mm X 700mm
Slab thickness	150mm
Grade of concrete	M20
Grade of steel	Fe500, Fe415

TABLE II Details of Loading

Frame Load	
All outer wall loading	12.44 kN/m
Balcony wall loading	2.6 kN/m
Toilet wall loading	6.5 kN/m

Shell Load	
Dead load	1.2 kN/m ²

Live Load on shells	
All rooms	2.5 kN/m ²
Toilet and bathrooms	2 kN/m ²
Corridors, passages	5 kN/m ²
Balconies	3 kN/m ²
Roof	1.5 kN/m ²

TABLE III Capacity Calculation of RCC Section

Width	300 mm
Depth	700 mm
Corner bars	16 mm
All other bars	12 mm
Area of steel A_{st}	1832 mm ²
% Steel	0.87%
Ultimate load carrying capacity P_u	2279.064 kN
Ultimate moment carrying capacity M_u	435.1 kNm

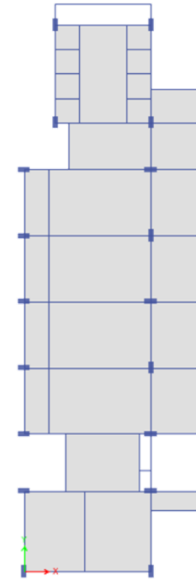


Fig. 3 Plan View of Building Modal

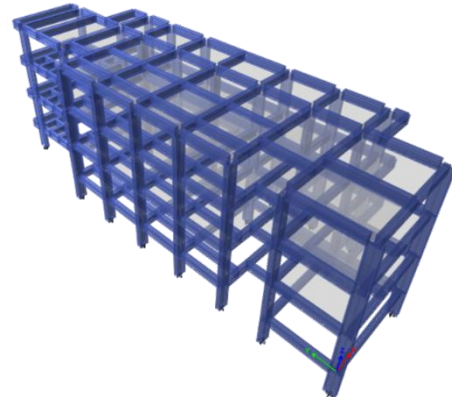


Fig. 4 3-D View of Building Modal

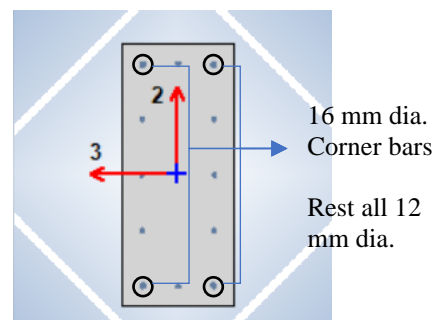


Fig. 5 Cross-Sectional Details of RCC

IV. FINITE ELEMENT MODELLING

A. Part Module

The proposed FE model consists of three main parts: Outer steel tube, Sandwiched concrete infill & Inner steel tube. All sections are defined as 3D solid sections and are deformable body. Size of the Circular section is to be determined by trial-and-error method so as to match the load carrying capacity of the RCC column used in the building. That is matched when outer tube diameter is kept as 250 mm and inner tube diameter as 150 mm with thickness of both tubes kept as 6mm and length of column is taken as 3150mm which is same as the story height in the building.

B. Material Modelling of Structural Steel

Different stress (σ)–strain (ϵ) models have been used for the steel material by different researchers, including the elastic-perfectly plastic model, and the elastic-plastic model with linear hardening or multi-linear hardening. Here for the sake of simplicity and to reduce material complexity the bi-linear stress-strain curve for structural steel is used. To model accurate behaviour of cold formed steel the Ramberg-Osgood material model is used. The Ramberg-Osgood model entails developing the engineering stress-strain curve, which is subsequently rectified to the real stress-strain curve. The steel material is treated as an elastic material in the FE analysis until it reaches its yield stress. The substance is then simulated as a plastic material. The equation by which this material has been modelled is as follows,

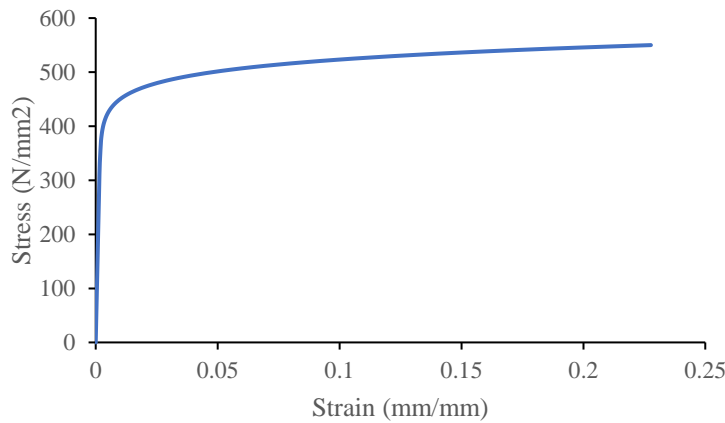


Fig. 6 Typical Ramberg-Osgood stress-strain curve for structural steel

$$\epsilon = \frac{\sigma}{E} + 0.002 \left(\frac{\sigma}{F_{ty}} \right)^{1/n}$$

where σ is the stress value, E is the material's elastic modulus, F_{ty} is the material's tensile yield strength, and n is the material's strain hardening exponent, which can be calculated using the following equation,

$$n = \frac{\log \left(\frac{\sigma_2}{\sigma_1} \right)}{\log \left(\frac{\epsilon_2}{\epsilon_1} \right)}$$

The modulus of elasticity (E_s) is taken as 200 GPa as per Indian Standards for structural steel and the Poisson's ratio (ν) is taken as 0.3.

C. Material Modelling of Sandwiched Concrete

Modelling of concrete material is most important part as the confinement effect is introduced here because of the two steel tubes when loaded provides the confinement to concrete infill between those two concentric tubes which in turn results in higher compressive strength of concrete than characteristics strength of concrete. This confinement effect of sandwiched concrete is accurately modelled by the material model given by Zhao which is known as Zhao model. Zhao model consist of following equation:

$$\sigma_{concrete} = \frac{f_{cc} \left(\frac{\epsilon}{\epsilon_{cc}} \right)}{r_m - 1 + \left(\frac{\epsilon}{\epsilon_{cc}} \right)^{r_m}}$$

$$f_{cc} = f_c \left[1 + \left(\frac{t_o}{D_o} \right) \left(\frac{f_{yo}}{f_c} \right) \right]$$

$$\varepsilon_{cc} = \varepsilon_{co} \left[1 + 5 \left(\frac{f_{cc}}{f_c} - 1 \right) \right]$$

$$\varepsilon_{co} = 0.002 + 0.001 \frac{f_c - 20}{80}$$

$$r_m = \frac{E_c}{E_c - E_{sec}}$$

$$E_c = 3320\sqrt{f_c} + 6900$$

$$E_{sec} = \frac{f_{cc}}{\varepsilon_{cc}}$$

$$f_c = \gamma_c f_c$$

$$\gamma_c = 1.85D_c^{-0.135} \quad (0.85 \leq \gamma_c \leq 1.0)$$

The model calculated by these equations can be represented by figure 7 with the following properties. This model given by Zhao is proven to give accurate stress-strain relationship called Engineering stress-strain relationship and it is verified with experimental results by Zhao et al. (2002).

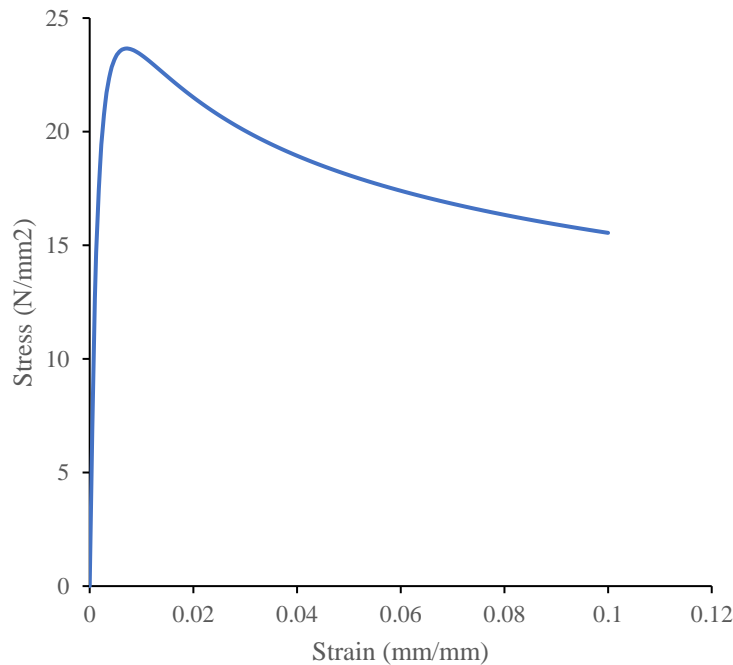


Fig. 7 Zhao Model for Sandwiched Concrete



Fig. 8 Assembled CFDST column

D. Step Module

In this module the step for the FE analysis was given as Dynamic-Explicit analysis. In this step the time period of the analysis was set as 1 sec. with increment value of time scaling factor as 0.2 sec. Mass scaling was introduced so as to reduce the analysis time with semi-automatic time scaling on whole model at the beginning of the step with scale factor as 10.

E. Interaction Module

In the ABAQUS models, the interactions were surface-to-surface contacts. Two interactions were required for each model. The first was between the outer tube and the concrete section, where the outer tube's inner sides served as the master surface while the concrete's outer faces served as the slave surface. The second interaction takes place between the inner concrete faces (master surface) and the inner tube's outer faces (slave surface). The contact pressure-overclosure model was utilized in the normal direction, and "normal behaviour" was selected as a "hard contact." The Coulomb friction model was used in tangential directions to the surface.

Multi-point constraints (MPCs) allow constraints to be imposed between different degrees of freedom of the model; and can be quite general (nonlinear and nonhomogeneous). The most required constraints are available directly by choosing an MPC type and giving the associated data. MPC Beam connection provides a rigid beam between two nodes to constrain the displacement and rotation at the first node to the displacement and rotation at the second node, corresponding to the presence of a rigid beam between the two nodes. In these models, MPC Beam type connection is defined at top and bottom surface connecting all the nodes of steel and concrete to act as rigid plate.

F. Boundary Condition and Loading Module

Total 3 boundary conditions were applied in the FE model. The first condition is fixed RP-2 at the origin with displacement/rotation type being $U1=U2=U3=UR1=UR2=UR3=0$. The second boundary condition, which similarly employed the displacement/rotation type, was used to allow RP1 to move being $U1=U2=UR3=0$. The third boundary condition, which set the value of $U3$ to 20, caused the column to be compressed in -Z direction.

G. Mesh Module

Both the steel tubes and sandwiched concrete of the CFDST were modeled using eight-node three dimensional solid elements with reduced integration (C3D8R), with three translation degrees of freedom at each node. Mesh size is taken as 20 mm for both steel tubes as well as sandwiched concrete so as to assign a good connection between both as shown in figure after performing mesh convergence analysis.

H. Result of FE Modelling

After designing and analyzing the CFDST column the same procedure was repeated for the CFST column with outer steel tube diameter being 250 mm and thickness being 6 mm with concrete core of 238 mm. This column was designed and analyzed by the same FE parameters and normalized interaction curve is prepared as given in figure.

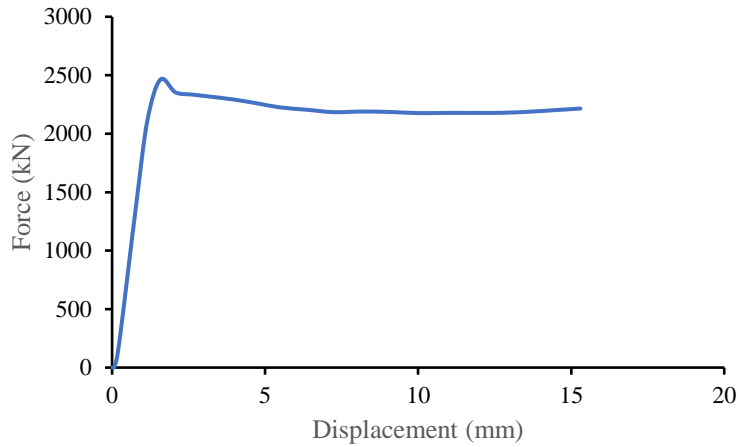


Fig. 11 Axial Force vs Displacement Curve

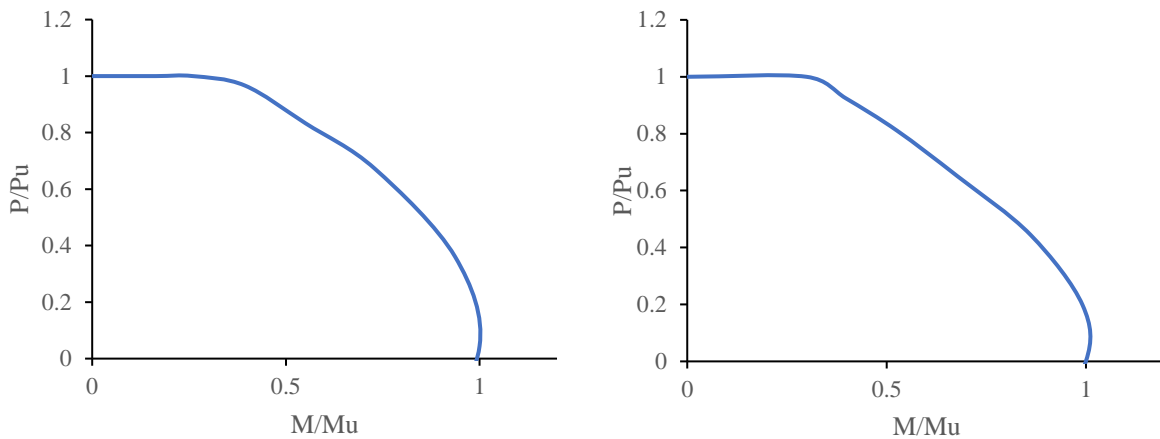


Fig. 10 Normalized Interaction curve of CFDST column Fig. 9 Normalized Interaction curve of CFST column

V. RESULTS AND DISCUSSION

Replacement of RCC columns by CFDST column with the same ultimate capacity was done. For the comparison purpose replacement of RCC column by CFST column is also analyzed. After completion of analysis the loadings (Axial loading) and moments (M 3-3) data were studied so as to ensure the safety of CFST and CFDST columns. These data were then checked by the interaction curve as ETABS does not provide checking for composite column sections. Loads and Moments on all 24 columns are given in table.

TABLE IV Loadings and Moments on all CFDST and CFST columns used in building

CFDST Column Force at Ground level		
Column Label	P (kN)	M3-3 (kN-m)
C1	174.6134	124.5696
C2	171.1429	113.7918
C3	186.7342	125.6676
C4	139.6854	166.9323
C5	157.0798	120.5805
C6	159.4564	161.7267
C7	248.4626	135.5943
C8	107.3805	115.7066
C9	115.6189	133.2887

CFST Column Force at Ground level		
Column Label	P (kN)	M3-3 (kN-m)
C1	175.3619	140.33
C2	172.5218	144.4674
C3	186.589	126.6063
C4	130.7765	134.2845
C5	154.432	125.6652
C6	152.0255	133.7853
C7	243.73	140.2683
C8	109.2252	144.3244
C9	107.3831	152.3734



C10	285.6357	128.7322
C11	100.5458	111.5905
C12	4.6125	136.5766
C13	107.9986	116.8883
C14	115.7374	133.3367
C15	285.4205	128.8747
C16	152.4341	123.5869
C17	151.3168	165.7669
C18	254.2802	135.7967
C19	105.4507	134.05
C20	160.8683	121.4185
C21	183.171	112.0234
C22	189.3971	119.8444
C23	260.3863	121.7855
C24	261.4033	120.2621

C10	279.2289	135.2093
C11	102.1806	141.8463
C12	5.0325	134.658
C13	110.0834	144.3507
C14	107.5458	154.1293
C15	279.3278	136.7546
C16	149.5859	125.7114
C17	143.6834	134.3821
C18	249.9277	144.1821
C19	98.1208	170.7819
C20	163.1724	141.816
C21	183.0948	159.5124
C22	190.1668	156.698
C23	256.529	152.225
C24	256.6185	146.444

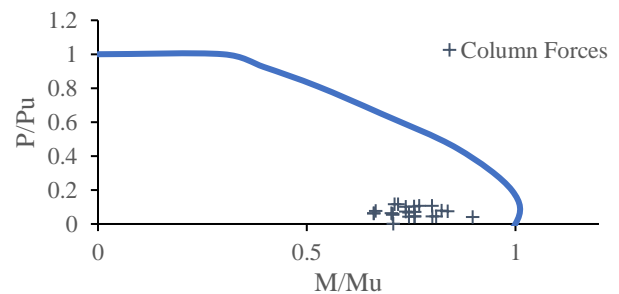
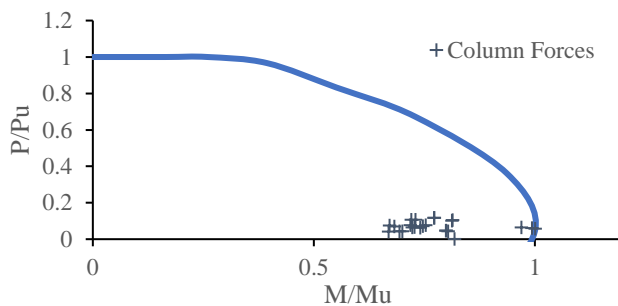


Fig. 13 Normalized Interaction Curve of CFDST column with Column Forces

Fig. 13 Normalized Interaction Curve of CFST column with Column Forces

Verification of all the column forces has been done by the interaction curve prepared as shown in figure 6.2 and 6.3. All CFST and CFDST column forces are represented by '+' marks in figure. All points are positioned below the interaction curve hence we can say that all CFST and CFDST columns are safe for provided loadings.

AXIAL FORCE

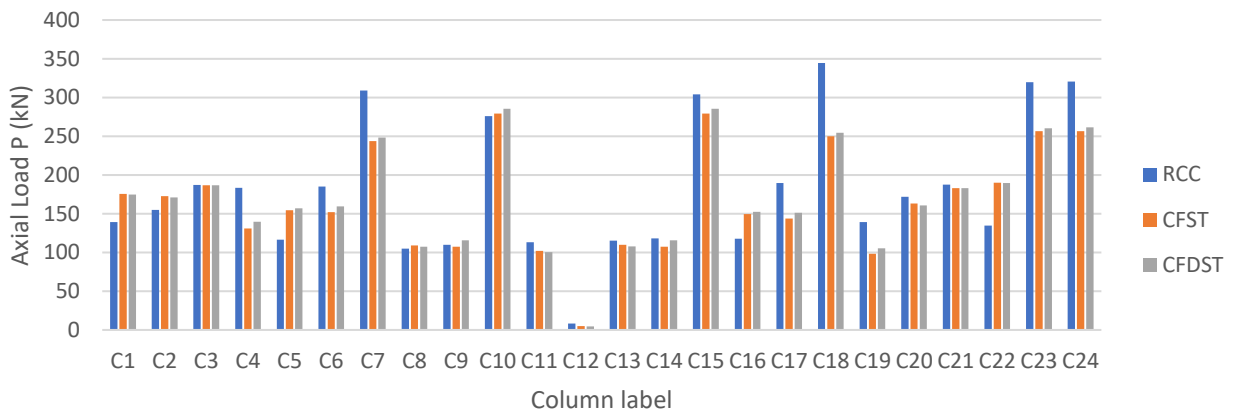


Fig. 14 Comparison of Axial Force Carried by Columns

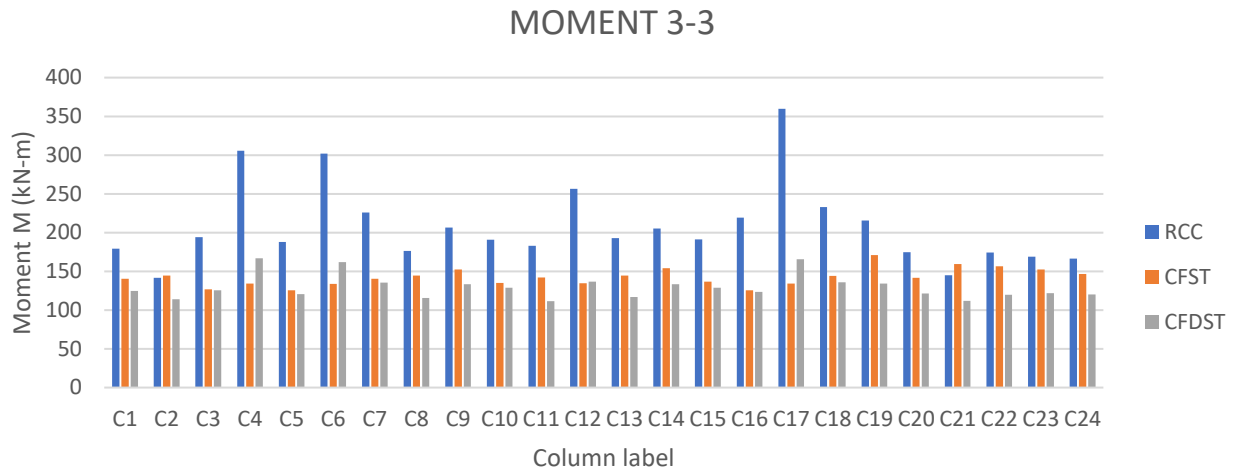


Fig. 15 Comparison of Moments Carried by Columns

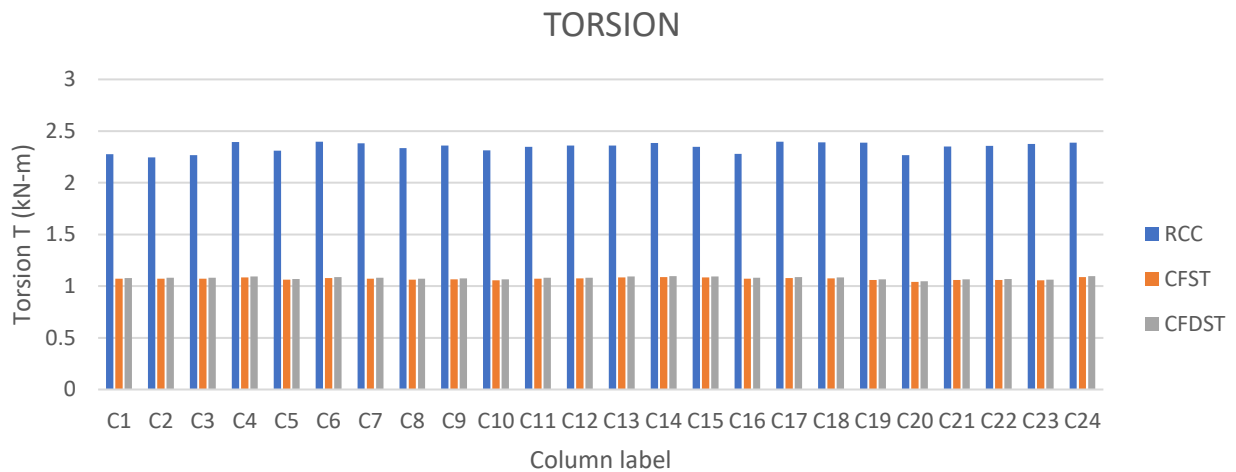


Fig. 16 Comparison of Torsional Moments Carried by Columns

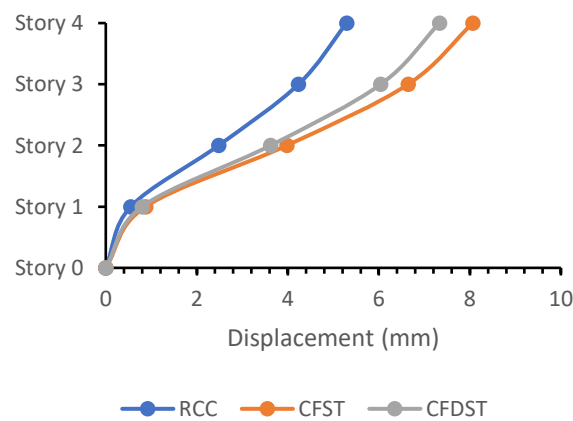


Fig. 17 Story Displacement-EQ Loading

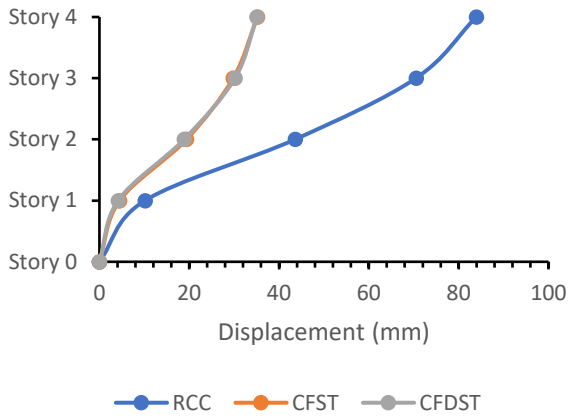


Fig. 18 Story Displacement-TH_COALINGA

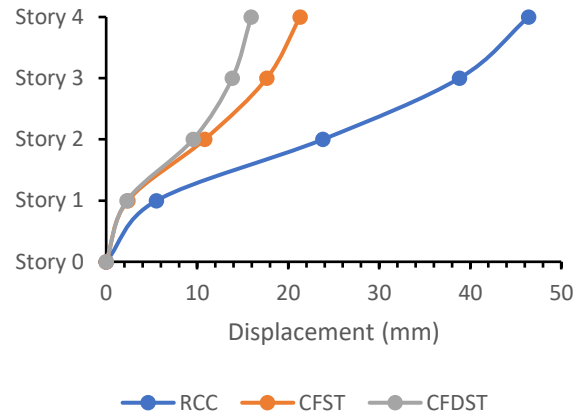


Fig. 19 Story Displacement-TH_IMPERIALVELLY

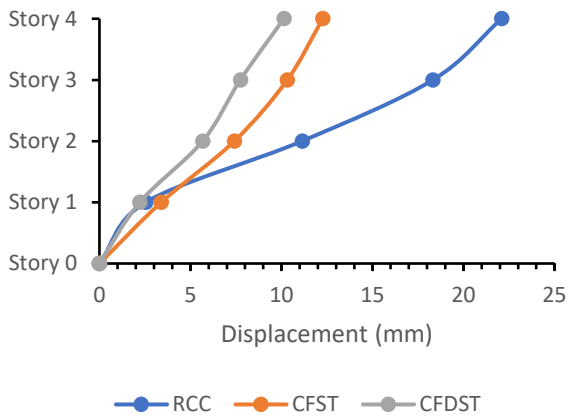


Fig. 20 Story Displacement-TH_MORGANHILL

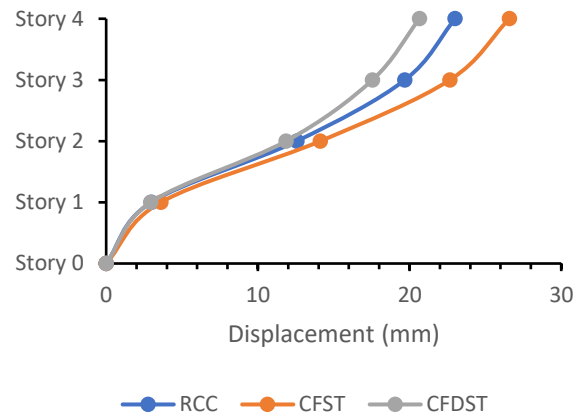


Fig. 21 Story Displacement-TH_NORTHRIDGE

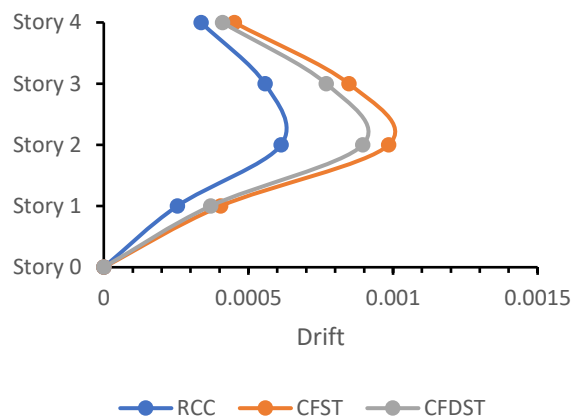


Fig. 22 Story Drift-EQ Loading

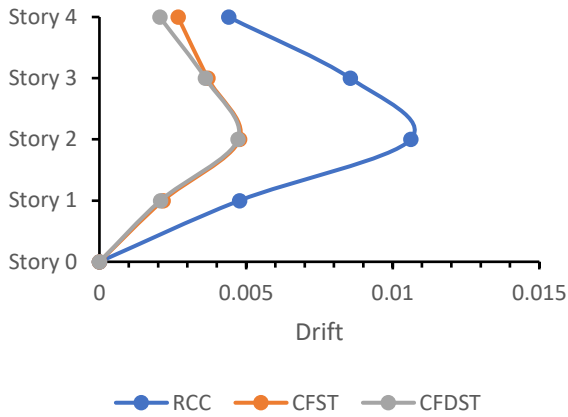


Fig. 23 Story Drift-TH_COALINGA

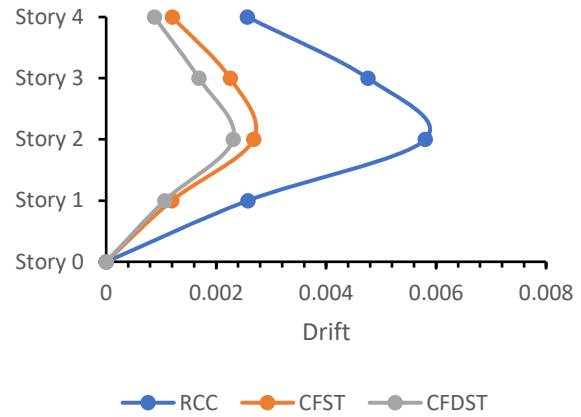


Fig. 24 Story Drift-TH_IMPERIALVELLY

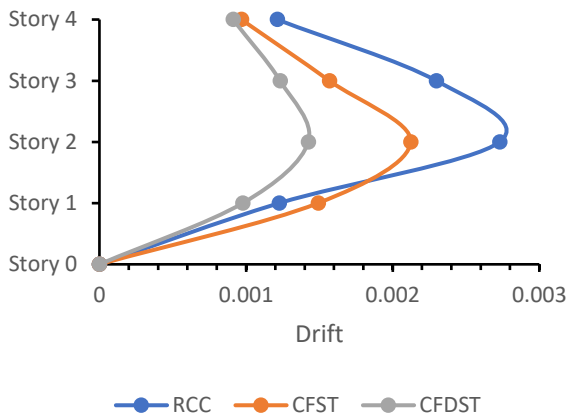


Fig. 25 Story Drift-TH_MORGANHILL

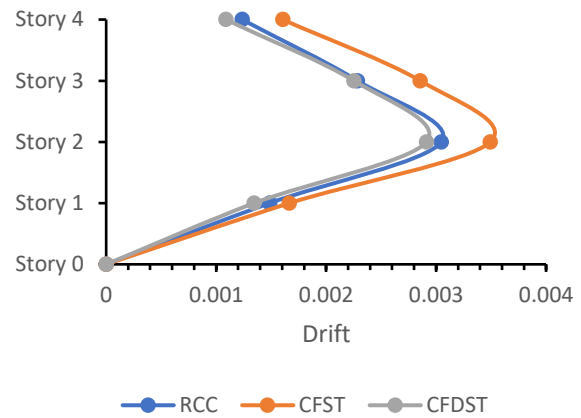


Fig. 26 Story Drift-TH_NORTHTRIDGE

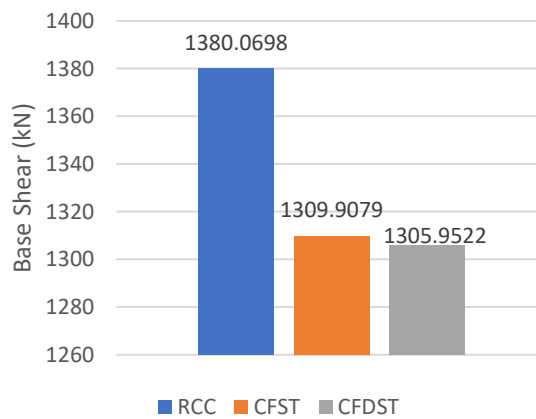


Fig. 27 Base Shear-EQ Loading

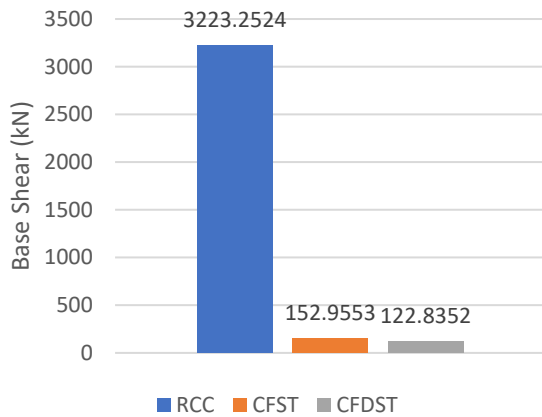


Fig. 28 Base Shear-TH_COALINGA

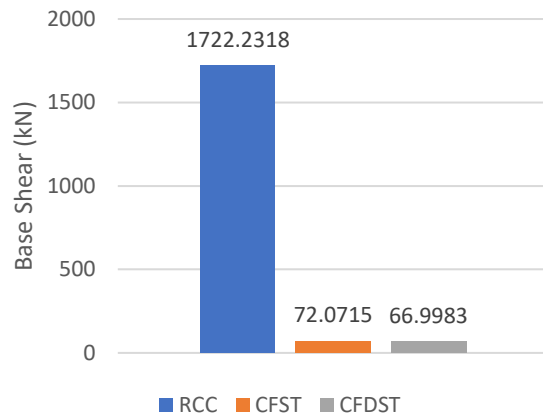


Fig. 29 Base Shear-TH_IMPERIALVELLY

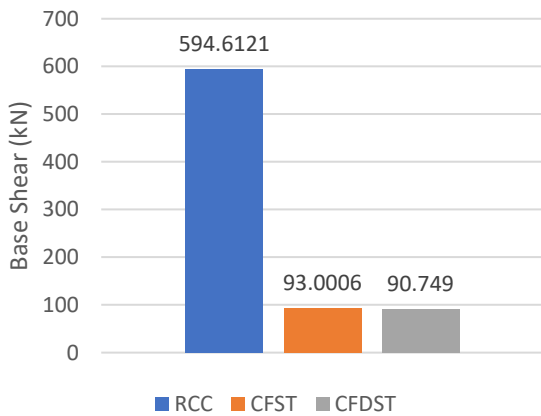


Fig. 30 Base Shear-TH_MORGANHILL

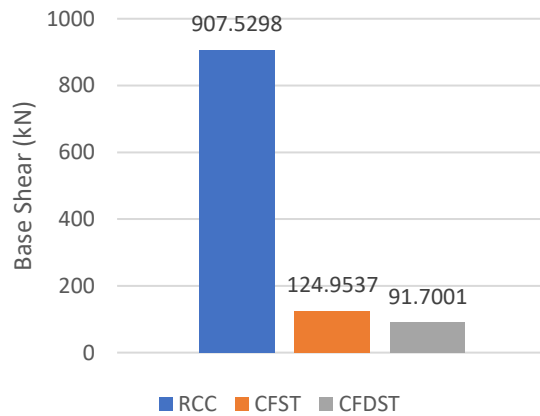


Fig. 31 Base Shear-TH_NORTHBRIDGE

A. Discussion

- Result values of axial loads and moments when presented on the interaction curve all points are under the interaction curve. Hence all the columns (CFST and CFDST) can be considered as safe under working loads.
- Axial force comparison is done from the model studied and it can be seen that when we compare CFDST column with RCC column, we have on an average 15% - 16% axial force reduction with maximum being 44%.
- When we compare the moments which are present on columns it is noted that compare to RCC, CFDST columns have 35% -37% average moment reduction with maximum moment reduction being 54% for current model studied.
- As the same when torsion of CFDST compared with RCC average reduction found out is of 53% with maximum torsion reduction being 55%.
- When these same comparison of CFDST Column with CFST column is made average reduction of axial force, moments and torsion is found to be 3%, 8.5% and -1% respectively. (-1% shows that CFST column has lower torsional moments than CFDST column)
- When the static loading is considered, performance of CFDST column is not quite up to expectations compared to RCC column. But when compared to CFST column, CFDST column gives improved results which is lesser story displacements about 10%.
- When the building model is subjected to non-linear time histories as described before, story displacements are reduced about 40% to 60% with an average of 43% story displacement when CFDST columns are being compared with RCC columns.
- For the same non-linear time history analysis, when the comparison has been made between CFDST column and CFST column on an average 15% - 16% reduction of story displacement is found.
- When static loading is taken into account, the performance of the CFDST column falls short of expectations when compared to the RCC column. However, when compared to the CFST column, the CFDST column produces better results, with around 10% fewer story drifts.

- When CFDST columns are compared to RCC columns, story drifts are reduced by roughly 35% to 65% with an average of 40% when the building model is subjected to non-linear time histories as detailed previously.
- When comparing the CFDST column to the CFST column for the identical non-linear time history analysis, a 18% reduction in story drift is seen on average.
- Performance of CFDST column under static loading when base shear is considered is in contrast of other parameters studied before. Here while comparing RCC and CFDST columns the base shear is reduced up to 5.4% and compared to CFST columns, reduction can be seen as 0.5%.
- Now as we talk about non-linear time history, base shear of CFDST column is drastically reduces when compared to RCC column by almost 90% and when compared to CFST column this reduction is around 14%.
- This is the result of lesser weight as compared to RCC and CFST both columns and time period of this CFDST column is much higher then RCC column, which is roughly 40% - 50%.

VI. CONCLUSION

This research project has made significant contribution in knowing and understanding behaviour of CFDST columns under combine loading and moments. Conclusions of the work are summarized as follows:

- CFDST columns exhibits more ductile behaviour than RCC because the presence of hollow portion.
- Higher strength of CFDST columns can be achieved by comparatively larger hollow ratios.
- Using materials with higher strength isn't significant way to improve performance of CFDST column.
- On the use of CFDST columns instead of RCC columns, increment of 45% - 50% is observed in time period.
- Mass reduction of almost 10% is achieved by using CFDST columns, so in the earthquake prone area lesser mass is proven to be safer than having more mass of structure.
- Small amount of axial force reduction can be achieved by using CFDST columns in place of RCC columns.
- While using the CFDST column, significant reduction in the moments present in the column is seen.
- Torsional moments seem to cut back in half amount, so in irregular buildings where the torsion is dominant using this CFDST columns can be beneficial.
- As far as static loading is considered, CFDST columns are not suitable to replace RCC columns.
- Better seismic performance can be achieved because of lesser weight and improved energy dissipation mechanism, which can be seen by the results of story displacements, story drifts and base shear.
- When CFDST column's performance is compared with CFST column's performance better seismic performance, load carrying capacities, moment carrying capacities and energy absorptions can be achieved.
- As far as column forces are considered capacity of CFDST and CFST columns are nearly same for axial loadings as well as torsional moments but while carrying the moments CFDST column section has showed improved performance than CFST column sections.
- Under the static loading conditions performance of CFDST column is better than CFST column section in story displacement, story drifts and base shears because of lesser weight and higher confinement effect due to the presence of an extra inner steel tube.
- When the non-linear time histories are considered CFDST column section has always proven to be better option than CFST columns.

REFERENCES

- [1]. Ahmed, M., Liang, Q. Q., Hamoda, A., & Arashpour, M. (2022). Behavior and design of thin-walled double-skin concrete-filled rectangular steel tubular short and slender columns with external stainless-steel tube incorporating local buckling effects. In *Thin-Walled Structures* (Vol. 170). <https://doi.org/10.1016/j.tws.2021.108552>
- [2]. Zhao, H., Wang, R., Lam, D., Hou, C. C., & Zhang, R. (2021). Behaviours of circular CFDST with stainless steel external tube: Slender columns and beams. *Thin-Walled Structures*, 158(April 2020), 107172. <https://doi.org/10.1016/j.tws.2020.107172>
- [3]. Saberi, H., Zadeh, V. K., Mokhtari, A., & Saberi, V. (2020). Investigating of the effect of concrete confinement on the axial performance of circular concrete filled double-skin steel tubular (CFDST) long columns. *Journal of Rehabilitation in Civil Engineering*, 8(3), 43–59. <https://doi.org/10.22075/JRCE.2020.19167.1362>
- [4]. Ding, F. xing, Wang, W. jun, Lu, D. ren, & Liu, X. mei. (2020). Study on the behavior of concrete-filled square double-skin steel tubular stub columns under axial loading. *Structures*, 23(July 2019), 665–676. <https://doi.org/10.1016/j.istruc.2019.12.008>
- [5]. Ahmed, M., Liang, Q. Q., Patel, V. I., & Hadi, M. N. S. (2020). Computational simulation of eccentrically loaded circular thin-walled concrete-filled double steel tubular slender columns. *Engineering Structures*, 213(February), 110571. <https://doi.org/10.1016/j.engstruct.2020.110571>

- [6]. Vernardos, S., & Gantes, C. (2019). Experimental behavior of concrete-filled double-skin steel tubular (CFDST) stub members under axial compression: A comparative review. *Structures*, 22(June), 383–404. <https://doi.org/10.1016/j.istruc.2019.06.025>
- [7]. Wang, F., Young, B., & Gardner, L. (2019). Experimental Study of Square and Rectangular CFDST Sections with Stainless Steel Outer Tubes under Axial Compression. *Journal of Structural Engineering*, 145(11), 04019139. [https://doi.org/10.1061/\(asce\)st.1943-541x.0002408](https://doi.org/10.1061/(asce)st.1943-541x.0002408)
- [8]. Ipek, S., & Güneysi, E. M. (2019). Ultimate Axial Strength of Concrete-Filled Double Skin Steel Tubular Column Sections. *Advances in Civil Engineering*, 2019. <https://doi.org/10.1155/2019/6493037>
- [9]. Han, L.-H., Lam, D., & Nethercot, D. A. (2018). Design Guide for Concrete-Filled Double Skin Steel Tubular Structures. In *Design Guide for Concrete-Filled Double Skin Steel Tubular Structures*. <https://doi.org/10.1201/9780429440410>
- [10]. PT NU. (2018). *Structures*, #pagerange#. <https://doi.org/10.1016/j.istruc.2018.04.006>
- [11]. Hafezolgborani, M., Hejazi, F., Vaghei, R., Jaafar, M. S. Bin, & Karimzade, K. (2017). Simplified damage plasticity model for concrete. *Structural Engineering International*, 27(1), 68–78. <https://doi.org/10.2749/101686616X1081>
- [12]. Gore, V. V., & Kumbhar, P. D. (2016). Comparative Behavioural Study of Multi Storied Building Provided with RCC and Concrete Filled Steel Tube Columns. *Proceedings of the 2nd National Conference for Engineering Post Graduate Students, RIT NConPG-16, May, 219–224*.
- [13]. Wang, R., Han, L. H., Zhao, X. L., & Rasmussen, K. J. R. (2016). Analytical behavior of concrete filled double steel tubular (CFDST) members under lateral impact. *Thin-Walled Structures*, 101, 129–140. <https://doi.org/10.1016/j.tws.2015.12.006>
- [14]. Elchalakani, M., Karrech, A., Hassanein, M. F., & Yang, B. (2016). Plastic and yield slenderness limits for circular concrete filled tubes subjected to static pure bending. *Thin-Walled Structures*, 109, 50–64. <https://doi.org/10.1016/j.tws.2016.09.012>
- [15]. Hassanein, M. F., & Kharoob, O. F. (2014). Analysis of circular concrete-filled double skin tubular slender columns with external stainless steel tubes. *Thin-Walled Structures*, 79, 23–37. <https://doi.org/10.1016/j.tws.2014.01.008>
- [16]. Pagoulatou, M., Sheehan, T., Dai, X. H., & Lam, D. (2014). Finite element analysis on the capacity of circular concrete-filled double-skin steel tubular (CFDST) stub columns. *Engineering Structures*, 72, 102–112. <https://doi.org/10.1016/j.engstruct.2014.04.039>
- [17]. Hassanein, M. F., & Kharoob, O. F. (2014). Compressive strength of circular concrete-filled double skin tubular short columns. *Thin-Walled Structures*, 77, 165–173. <https://doi.org/10.1016/j.tws.2013.10.004>
- [18]. Hassanein, M. F., Kharoob, O. F., & Liang, Q. Q. (2013). Circular concrete-filled double skin tubular short columns with external stainless steel tubes under axial compression. *Thin-Walled Structures*, 73, 252–263. <https://doi.org/10.1016/j.tws.2013.08.017>
- [19]. Hassanein, M. F., Kharoob, O. F., & Liang, Q. Q. (2013). Behaviour of circular concrete-filled lean duplex stainless steel tubular short columns. *Thin-Walled Structures*, 68, 113–123. <https://doi.org/10.1016/j.tws.2013.03.013>
- [20]. Tao, Z., Wang, Z. Bin, & Yu, Q. (2013). Finite element modelling of concrete-filled steel tub columns under axial compression. *Journal of Constructional Steel Research*, 89, 121–131. <https://doi.org/10.1016/j.jcsr.2013.07.001>
- [21]. Huang, F., Yu, X., & Chen, B. (2012). The structural performance of axially loaded CFST columns under various loading conditions. *Steel and Composite Structures*, 13(5), 451–471. <https://doi.org/10.12989/scs.2012.13.5.451>
- [22]. Uy, B., Tao, Z., & Han, L. H. (2011). Behaviour of short and slender concrete-filled stainless steel tubular columns. *Journal of Constructional Steel Research*, 67(3), 360–378. <https://doi.org/10.1016/j.jcsr.2010.10.004>
- [23]. Liang, Q. Q., & Fragomeni, S. (2009). Nonlinear analysis of circular concrete-filled steel tubular short columns under axial loading. *Journal of Constructional Steel Research*, 65(12), 2186–2196. <https://doi.org/10.1016/j.jcsr.2009.06.015>
- [24]. Tao, Z., Han, L. H., & Zhao, X. L. (2004). Behaviour of concrete-filled double skin (CHS inner and CHS outer) steel tubular stub columns and beam-columns. *Journal of Constructional Steel Research*, 60(8), 1129–1158. <https://doi.org/10.1016/j.jcsr.2003.11.008>
- [25]. Hu, H. T., Huang, C. S., Wu, M. H., & Wu, Y. M. (2002). Numerical Analysis of Concrete-Filled Steel Tubes Subjected to Axial Force. *Proceedings of the International Offshore and Polar Engineering Conference*, 12(1998), 73–80.
- [26]. Zhao, X. L., Han, B., & Grzebieta, R. H. (2002). Plastic mechanism analysis of concrete-filled double-skin (SHS inner and SHS outer) stub columns. *Thin-Walled Structures*, 40(10), 815–833. [https://doi.org/10.1016/S0263-8231\(02\)00030-7](https://doi.org/10.1016/S0263-8231(02)00030-7)
- [27]. Board, S. A. (n.d.). An ABAQUS Tutorial By a Student , For Students Courtesy of Austin Cox and the Undergraduate Aerospace.